Research Article

For reprint orders, please contact: reprints@futuremedicine.com

Regenerative Medicine

Development of a decellularized porcine bone matrix for potential applications in bone tissue regeneration

Ziyan Nie[‡,§,1], Xuesong Wang[‡,2], Liling Ren[1] & Yunqing Kang[*,2,3,4]

[1]School of Stomatology, Lanzhou University, Lanzhou, Gansu 730000, China

[2]Department of Ocean & Mechanical Engineering, College of Engineering & Computer Science, Florida Atlantic University, Boca Raton, FL 33431, USA

[3]Department of Biomedical Science, College of Medicine, Florida Atlantic University, Boca Raton, FL 33431, USA

[4]Integrative Biology Program, Department of Biological Science, College of Science, Florida Atlantic University, Boca Raton, FL 33431, USA

*Author for correspondence: kangy@fau.edu

[‡]Authors contributed equally

[§]Author was a visiting student at FAU

Aim: The objectives of this study were to develop a new decellularized bone matrix (DBM) and to investigate its effect on the *in vitro* cell behavior of human bone marrow-derived mesenchymal stem cells (hMSCs), compared with porous β-tricalcium phosphate (β-TCP) scaffolds. **Materials & methods:** Triton X-100 and deoxycholate sodium solution, combining DNase I and RNase, were used to decellularize porcine bones. The DBM were then characterized by DNA contents and matrix components. hMSCs were then seeded on the DBM and β-TCP scaffolds to study cell behavior. **Results:** Results showed that most porcine cells were removed and the matrix components of the DBM were maintained. Cell culture results showed that DBM promoted cell attachment and proliferation of hMSCs but did not significantly promote the gene expression of osteogenic genes, compared with β-TCP scaffolds. **Conclusion:** DBM has similar function on cell behavior to β-TCP scaffolds that have promising potential in bone tissue regeneration.

Graphical abstract:

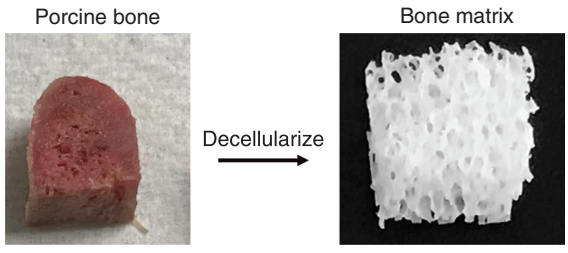

First draft submitted: 28 September 2019; Accepted for publication: 2 May 2020; Published online: 22 May 2020

Keywords: β-TCP scaffold • bone marrow • craniofacial bone regeneration • decellularization • extracellular matrix • mesenchymal stem cells • osteogenesis • porcine bone • tissue engineering • xenogeneic cells

The repair of large craniofacial bone defects still faces major challenges not only because of the complexity of craniomaxillofacial bones, but also due to the lacking of a functional, off-the-shelf, bone-grafting material [1,2]. Current bone-grafting materials including autografts and allografts. They have their respective advantages and drawbacks in bone regeneration [3,4]. Although autografts are the gold standard for bone regeneration, their application in bone regeneration is hampered by the limited supply of donor bone and considerable donor site

Future Medicine

morbidity [5]. Allografts are an alternative bone-grafting material to autografts. However, its potential risk of immune rejection and disease transmission also limits its application in craniofacial bone regeneration [6]. In recent years, synthetic bone-grafting materials, including organic and inorganic scaffold materials, have been extensively studied in bone tissue regeneration [7]. However, the applications of synthetic ceramic bone cements or polymer scaffolds were hindered in craniofacial bone defects due to insufficient vascularization and limited bone integration [8]. More attention has been paid to decellularized xenografts during the past decade due to their native extracellular matrix and structure [9].

Decellularized scaffolds, which are derived from native tissues and organs, can provide a biological material with original protein components and ultrastructure of the extracellular matrix (ECM) for tissue engineering [10,11]. Decellularized tissues, including skin, bladder, cornea, blood vessels, heart valves, liver, nerves, tendons and cartilage have been extensively studied in regenerative medicine [11–13]. Decellularized bone matrix (DBM) has also been developed as a scaffold for bone tissue engineering due to its three-dimensional structure and biomechanical properties [14]. The decellularized bone ECM can provide structural support for stem cells and interact with them to guide bone regeneration [15]. Currently, most decellularized bone matrixes are obtained from rats or bovine [9,16–19]. Some studies reported that porcine-derived bones had been decellularized to produce porcine-derived DBM [20,21]. *In vivo* studies showed that porcine-derived DBM promoted cell infiltration and new blood vessel formation were achieved after 6 months [22], and the porcine-derived DBM maintained its osteoinducive properties after implanted in mice subcutaneous pockets [20]. In addition, an *in vivo* study demonstrated that decellularized bone matrix loaded with rat mesenchymal stem cells (MSCs) can induce the regeneration of cranial defects in rats [13]. These studies indicate the promising potential of porcine-derived DBM scaffold in bone tissue engineering. Most importantly, porcine species is the genetically closest one to the human being and porcine bone is abundant and easily obtained [23].

However, to produce a biocompatible DBM, complete removal of xenogeneic cells is crucial and also challenging. Currently, the techniques for decellularization include physical methods, chemical methods and the combination of enzymic preparations [24]. Physical methods refer to the freeze–thaw cycle treatment, mechanical agitation and sonication. Chemical reagents include acid–base solutions, hypotonic and hypertonic solutions, detergents and ethanol [10,25]. However, while these methods may work well on soft tissues or organs, challenges remain in decellularizing hard tissues like bone. There are no standardized decellularization protocols to decellularize large porcine bones for bone defect regeneration. Furthermore, the effect of the decellularized porcine bone matrix on the *in vitro* osteogenesis of human bone marrow mesenchymal stem cells (hMSCs) had not been investigated, and whether this mimetic DBM would have better or similar osteogenic properties than/to a synthetic bioceramic scaffold, β-TCP that is widely used in bone tissue regeneration, is unknown.

Therefore, in this study we modified previously published decellularized methods to develop a new decellularization method for porcine bone. This method combined physical, chemical, and enzymatic methods to decellularize porcine bones with large size. DBM was then fully characterized. Native bone matrix (NBM) before decellularization served as a control group. We then investigated the ability of the DBM to promote the osteogenic differentiation of hMSCs. As a comparison, we used a synthetic material β-TCP scaffold to compare their osteogenic ability. Calcium and phosphorus ions are the main inorganic components of hard tissues of vertebrates. Calcium phosphate ceramics are widely studied for bone regeneration. Calcium phosphate ceramics have no risk of disease transmission or immunogenic response and is easy to sterilize and store. It is also a potential carrier of living cells and growth factors. The most common bioceramic material, β-TCP scaffold has been extensively studied by many research groups and also our lab [26,27]. It has been approved to be used in clinical applications for bone filler due to its outstanding mechanical properties and biocompatibility. It is a promising scaffold material for bone tissue engineering [28]. Based on its good biocompatibility and osteogenesis of β-TCP, in this study we compared the cell attachment, proliferation, differentiation of hMSCs on DBM (the native-derived bone matrix) and β-TCP (the synthetic scaffold) that contains similar inorganic components. The objective of this current study was to investigate whether the new decellularization method can effectively obtain a biomimetic bone matrix and whether the DBM has similar or better pro-osteogenic properties than a synthetic β-TCP scaffold.

Materials & methods

Materials

Triton X-100 was obtained from EMD Millipore (MA, USA). Sodium deoxycholate was purchased from Sigma-Aldrich, MO, USA. DNase I and RNase were from Thermo Fisher Scientific (MA, USA) for the decellularization.

Primary antibody Collagen type I was purchased from Abcam, MA, USA and secondary antibody Biotinylated Horse Anti-Mouse IgG was purchased from Vector Lab, CA, USA. β-TCP powder was purchased from Nanocerox, Inc. (MI, USA). hMSCs were obtained from American Type Culture Collection (ATCC; VA, USA).

Decellularization of porcine bone matrix

Fresh porcine-derived ribs were obtained from a local food market. Soft tissues on the ribs were removed, and cortical bone was excised using a MOPEC Autopsy Saw (MI, USA), leaving the part of spongy bone. The spongy bone was then dissected into cubic pieces with 5 mm length, 5 mm width and 3 mm thickness. Some other shapes like cylinder, pyramid and wedge shapes were also produced for decellularization to demonstrate the potential of the new decellularization method. The bone samples were stored at -80°C until used.

After thawing the frozen bone samples overnight at 4°C, the thawed samples were heated at 60°C for 15 min and sonicated to remove fat tissue or lipids, and then washed with 60°C water three-times. The samples were then put into 1 × phosphate-buffered saline solution (PBS; Fisher Scientific, NH, USA) containing 1% Triton X-100 (EMD Millipore) and 0.5% sodium deoxycholate (Sigma-Aldrich) for 48 h at room temperature. Triton X-100 and sodium deoxycholate were effective detergents, which can disturb cell membranes and dissociate DNA from proteins, so they effectively removed cellular material from tissues. After washing several times with warm water, the samples were treated in DNase I (150 IU/ml) (EN0521, Thermo Fisher Scientific) and RNase (100 μg/ml) (EN0531, Thermo Fisher Scientific) for 24 h at 37°C. DNase I and RNase were able to degrade nucleic acid sequences, thus helped removing nucleotides after cell lysis. The samples were washed with 60°C preheated water and then 100% ethanol to further wash out lipid residues. Finally, 70% ethanol followed by sterile PBS were used to sterilize the decellularized bone matrix for further characterization and cell culture.

Characterization

Morphologies

To observe the pore morphologies of the DBM, scanning electron microscopy (SEM) was used. Native bone matrix (NBM) before decellularization, serving as a control, and DBM after decellularization were fixed in 2.5% glutaraldehyde for 1 h at room temperature. After that, the samples were washed with PBS and dehydrated in a graded series of ethanol, then dried in the hood and sputter-coated with gold for observation under a benchtop SEM (JEOL, JCM-6000Plus).

Mechanical strength

To measure the compressive strength of the NBM and DBM (Zwick-Roell universal tension-compression machine Z50), the NBM and DBM were trimmed into small discs with 5 mm width, 5 mm thickness and 10 mm height. Before all measurements, both top and bottom side of each sample were polished to ensure they were parallel with each other. The length, width and height of each sample were measured as well before loading. The speed of crosshead was 0.5 mm/min, and loading pressure was kept applying to the samples until they got cracked. Three samples per group were measured and each test repeated twice.

DNA quantification

After washing NBM and DBM with PBS three-times, the samples were frozen in -80°C for 20 min or longer and then thawed completely in a water bath at 37°C. This freeze/thaw cycle was repeated three-times; 0.2% Triton X solution (EMD Millipore) was added into each sample and left at room temperature for 30 min. The samples were sonicated for 10 min using ultrasonic machine, rinsed several times and transferred all the cell lysate into a tube. The dsDNA concentration of the cell lysate was quantified using Quant-IT PicoGreen dsDNA assay kit (Invitrogen, CA, USA). The samples were read at 480/520 nm (excitation/emission) on a fluorescence spectrophotometer (Flx800, Biotek, VT, USA) and the amount of dsDNA was calculated by comparing the standard curves of the known dsDNA sample according to the manufacturer's instruction.

4′,6-diamidino-2-phenylindole & hematoxylin & eosin staining

For 4′,6-diamidino-2-phenylindole (DAPI) staining, NBM and DBM were fixed in 4% paraformaldehyde for 15 min, then stained with DAPI. For hematoxylin & eosin (H&E) staining (Sigma), NBM and DBM were fixed in 10% neutral buffered formalin for 24 h, then decalcified with 0.5M EDTA (Fisher Scientific, NH, USA),

dehydrated in a graded series of ethanol (70, 80, 90, 100%) and then embedded in paraffin and finally cut into 5 μm thick sections. The sections were then stained with H&E staining.

Characterization of collagen contents

The Masson Trichrome Stains kit (Sigma) was used to stain the collagen fiber in the 20 μm thick sections NBM and DBM. The Sirius Red/Fast Green Collagen Staining kit from Chondrex Inc. (WA, USA) was used to stain all types of collagen and non-collagenous proteins, and then calculated the amount of collagen and noncollagenous proteins following the manufacturer's instruction.

Immunohistochemical staining on collagen was performed on the 5 μm thick sections of NBM and DBM. The sections were deparaffinized and rehydrated. A citrate buffer (pH 6.0; Millipore) was used to retrieve antigen at 95–100°C for 20 min and cooled at room temperature. The sections were washed with PBS solution containing 0.5% Tween 20 and blocked with Bloxall blocking solution (SP-6000, Vector) in the dark at room temperature for 10 min. The sections were then washed and blocked in 10% bovine serum albumin for 1 hour at room temperature. Mouse monoclonal primary anti-Collagen type I (ab90395, Abcam) antibody was applied for 1 hour at room temperature. After wash, the secondary antibody (Biotinylated Horse Anti-Mouse IgG Antibody, Vector Labs) was applied for 30 min on the sections at room temperature, followed by incubating with ABC reagent (Vectastain PK-4000, Vector Labs) for 5 min at room temperature. Finally, sections were developed with DAB peroxidase substrate (SK-4100, Vector Labs) for 3 min. The pictures were then captured by a Nikon TE2000 microscope.

In vitro recellularization of DBM with hMSC

Preparation of β-TCP scaffolds

To compare with the DBM, synthetic bioceramic β-TCP scaffolds were prepared by using an established template-casting method [29–31]. Briefly, mixed β-TCP nano-powder, carboxymethyl cellulose powder, dispersant (Darvan C) together with distilled water while stirring to form the β-TCP slurry. Then, paraffin beads with sizes between 1000 and 1180 μm were filled within specially-made molds. Next, β-TCP ceramic slurry was casted into the molds and solidify in ethanol, followed by dehydration with a series of alcohol solutions. After completely dried, β-TCP green-bodies were fired at 1250°C for 3 h. Thus, porous β-TCP scaffolds were fabricated and polished to 5 mm long, 5 mm wide and 3 mm thick, the same size as DBM, then used for the following cell experiments. The crystalline phases, mechanical properties and other properties of the β-TCP scaffold had been fully characterized in our previous studies [29–31].

Cell culture of hMSCs

hMSCs were purchased from ATCC. The cells were derived from normal, human bone marrow. Human MSCs were cultured in MEM (Thermo Fisher) with 10% fetal bovine serum and 1% antibiotic under standard conditions (5% CO_2, 95% humidity and 37°C). The medium was changed every 3 days. When the number of cells reached 90% in the T75 flask, the cells were subcultured by 0.25% trypsin–EDTA and resuspended them in culture medium. Cells under nine passages were used in all the experiments.

Cell attachment

In order to study the cell attachment on the decellularized bone matrix, a 3D platform rotator (Fisher Scientific) was used to seed hMSCs on the DBM and β-TCP scaffolds. Three samples of each group were placed in low adherent 48-well plate. In the first experiment, 1 ml of hMSCs cell suspension in MEM with concentration of 2×10^5 cells/ml were added to each well to cover the scaffold completely. The well plate was then placed on the 3D platform rotator with 30 r.p.m. and incubated at 37°C with 5% CO_2. After 4 h, the DBM and β-TCP samples were transferred to new wells. The remaining media from each well were collected to a 15 ml centrifuge tube. The cells attached in the same well were trypsinized and the cell suspensions were then collected and added into the 15 ml centrifuge tube. The number of total cells in the collected suspension in the 15 ml tube was counted by using a hemocytometer. Finally, the cell attachment efficiency was determined by using the following equation: N = (A - B)/A, where N stands for the rate of cells attached, A stands for the number of cells initially seeded and B stands for the number of cells that were collected in the 15 ml tube. In this preliminary experiment, the result showed that the attachment efficiency on DBM was around 1.5-fold higher than that on β-TCP. To confirm this attachment efficiency, we designed a second experiment. We used different initial cell concentration of hMSCs suspension to

seed hMSCs on the DBM and β-TCP. Here, 1 ml of hMSCs cell suspension in MEM with concentration of 5×10^4 cells/ml were added to each β-TCP scaffold and 1 ml of hMSCs cell suspension in MEM with concentration of 3.3×10^4 cells/ml were added to each DBM. Thus, the cell numbers attached on the two types of scaffolds would be similarly close for all the following experiments.

Cell morphology on the DBM & β-TCP scaffolds

Morphologies of the hMSCs seeded on the DBM and β-TCP scaffolds were observed by SEM. After 7 days of incubation in the MEM medium, the samples were fixed in 2.5% glutaraldehyde for 1 h at room temperature. Next, the samples were washed with PBS and dehydrated in a graded series of ethanol, then dried in a hood, sputter-coated with gold and observed by SEM a benchtop SEM (JEOL, JCM-6000Plus).

Cell proliferation

Three samples of each group at each time point were put in low adherent 48-well plate. One milliliter of hMSCs cell suspension in MEM with concentration of 5×10^4 cells/ml were added to each DBM and 1 ml of hMSCs cell suspension in MEM with concentration of 7.5×10^4 cells/ml were added to each β-TCP scaffold. The well-plates were then shaken on a 3D platform rotator for 4 h. The medium was changed every two days. At the time points of 1, 3, 7 and 14 days, the samples were washed with PBS and preserved at -80°C. Then, three cycles of freeze/thaw in -80/37°C were performed on the samples, followed by submersion in 0.2% Triton X solution for 30 min at room temperature, and finally sonicated for 10 min on ice. Finally, the cell lysates were ready to be used to determine dsDNA content by a Pico Green assay (Invitrogen). The samples were read at 480/520 nm (excitation/emission) on a fluorescence spectrophotometer (Biotek, Flx800). The amount of dsDNA was calculated by comparing the standard curves of the known dsDNA sample according to the manufacturer's instruction.

Cell differentiation

The early osteogenic differentiation of hMSCs on the DBM and β-TCP scaffolds was assessed through ALP specific activity. After being shaken for 1 day, the medium was replaced to osteogenic differentiation medium (Lonza Co., GA, USA) and changed medium every 2 days. At the end of day 1, 5, 7, and 14, the cell lysate was obtained using the same method as that in the above section (DNA quantification). The protein content of samples was measured using a BCA Protein Assay kit (Thermo Scientific). To determine ALP, a working solution containing p-nitrophenyl phosphate (p-NPP; Sigma-Aldrich) was added into samples and then incubated for 3 h at 37°C. After incubation, the absorbance values of samples were obtained on a microplate reader (Spectra Max 190, Molecular Devices; CA, USA) at 405 nm wavelength. The ALP concentration of samples was calculated through a standard curve. The ALP specific activity was determined by normalizing ALP value of each sample to its protein concentration.

Quantitative real-time PCR

After incubation of 7 and 14 days, the cellular total RNA was extracted using a RNeasy mini kit (QIAGEN, Germantown, MD, USA). RNA concentration was measured by a nanodrop (Thermo Scientific). An iScript cDNA synthesis kit (BIO-RAD, CA, USA) was used to reverse-transcribe RNA into cDNA. Then using cDNA product template, specific primers and iQ- SYBR Green supermix (BIO-RAD) in a total volume of 10 µl were performed real-time PCR on an AriaMx Real-Time PCR System (Agilent Technologies, CA, USA). Primer sequences are shown in Table 1, including *runx2*, *alp*, *oc*, *bsp* and *GAPDH*, which were purchased from Invitrogen and used to evaluate gene expression [27,32]. The relative genes expression levels were analyzed using the $2^{-\Delta\Delta Ct}$ method by normalizing with the housekeeping gene *GAPDH* as an endogenous control and calibrating with efficiency, where $\Delta\Delta C_t$ is calculated from $(C_t,\text{sample} - C_t,\text{control})_{\text{target gene}} - (C_t,\text{sample} - C_t,\text{control})_{\text{GAPDH}}$ [33].

Statistical analysis

The number of samples in each group was three and each experiment was repeated once. The statistical significance was analyzed by Analysis of variance (ANOVA) tests and Student's t-test by using GraphPad Prism. The value of $p < 0.05$ was considered statistically significant.

Table 1. Sequences of primers used for real-time PCR analysis.

Genes	Sequences
GAPDH	For: 50′-AACAGCGACACCCACTCCTC
	Rev: 50′-CATACCAGGAAATGAGCTTGACAA
alp	For: 50′-ACATTCCCACGTCTTCACATTT
	Rev: 50′-AGACATTCTCTCGTTCACCGCC
runx2	For: 50′-AGATGATGACACTGCCACCTCTG
	Rev: 50′-GGGATGAAATGCTTGGGAACT
bsp	For: 50′-ATGGCCTGTGCTTTCTCAATG
	Rev: 50′-GGATAAAAGTAGGCATGCTTG
oc	For: 50′-TGTGAGCTCAATCCGGACTGT
	Rev: 50′-CCGATAGGCCTCCTGAAGC

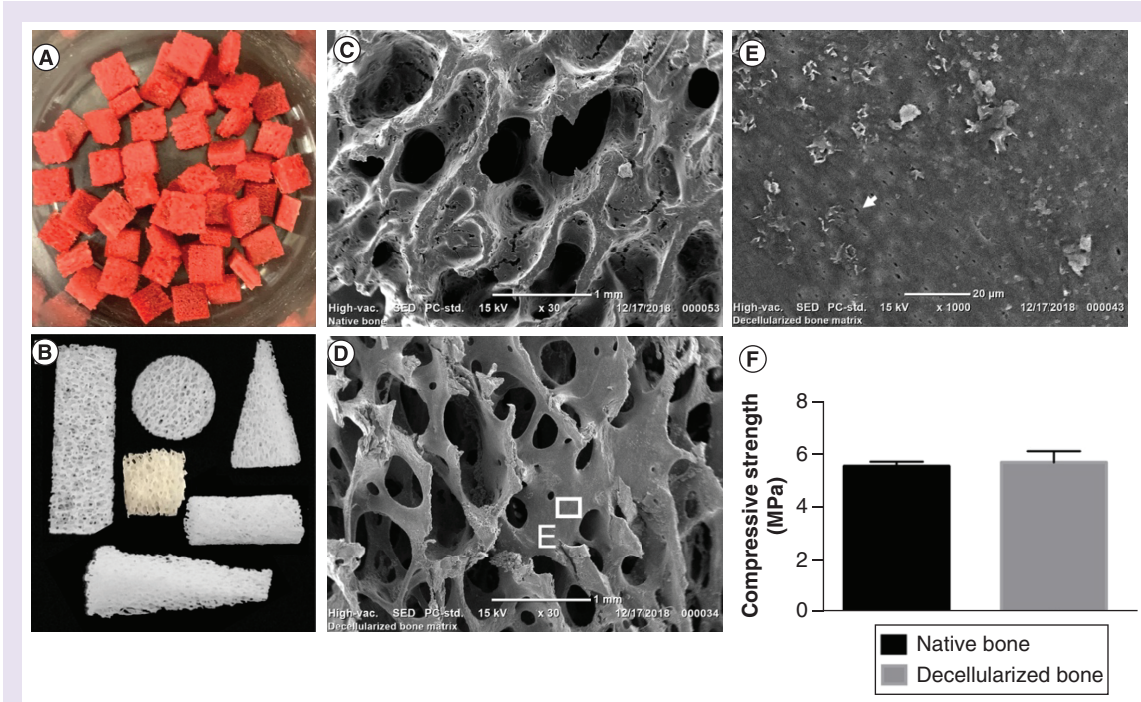

Figure 1. Morphology and mechanical strength of native bone matrix and decellularized bone matrix. Images show porcine fresh spongy bone of ribs **(A)** and various shapes of decellularized bone matrix **(B)**. scanning electron micrographs show porous architecture of native bone matrix before decellularization **(C)** and decellularized bone matrix **(D, E)**. Arrow shows the osteon micropore **(E)**. Mechanical strength between native bone matrix and decellularized bone matrix **(F)** ($p > 0.05$), N = 3, mean ± standard deviation. The error bars represent standard deviation.

Results

Morphologies & compressive strength of NBM & DBM

NBM was red in appearance and full of blood and marrows (Figure 1A). After decellularization, NBM became a white, porous appearance without any blood or marrow (Figure 1B). The porcine rib bones were biopsied into various kinds of types like cylinder, cuboid, cone and wedge and they were decellularized (Figure 1B). The cube with 5 mm length, 5 mm width and 3 mm thickness were used in all the experiments. SEM shows that DBM (Figure 1D) maintained the same porous microstructure of NBM (Figure 1C), implying decellularization process did not destroy the bone trabecular network. The pore sizes of DBM were around 500 μm. In the struts of the matrix, there are many micropores (arrow, Figure 1E). After decellularization, the mechanical strength was not changed dramatically. Before decellularization, the compressive strength of NBM was 5.59 ± 0.17 MPa, and after

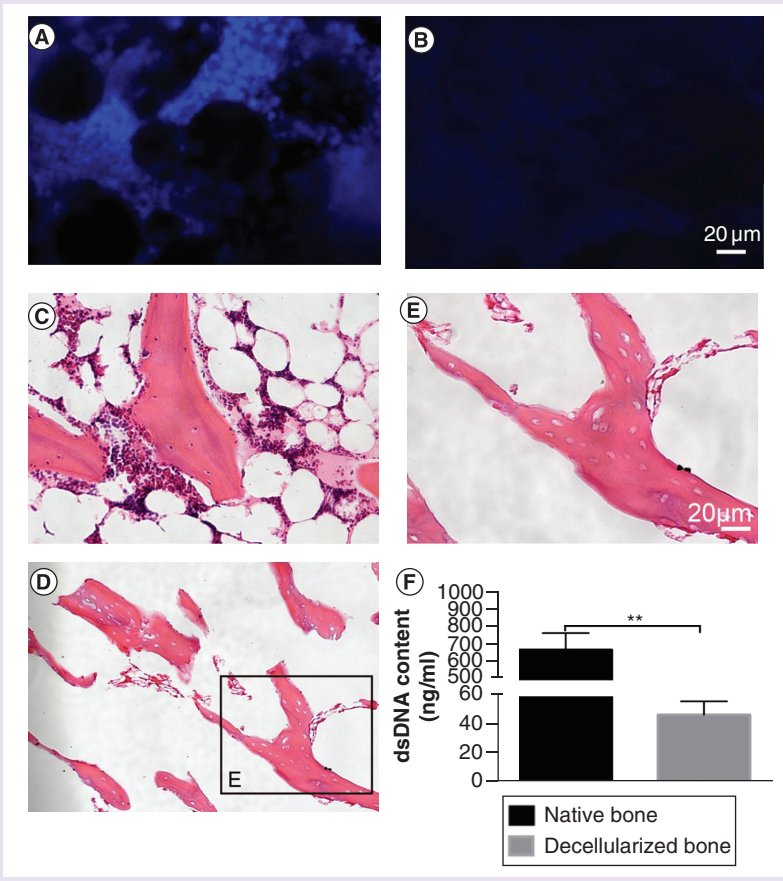

Figure 2. Histological analysis and dsDNA quantification. (A) DAPI staining shows native bone matrix has a large number of cell nucleus. **(B)** After decellularization, few cell nuclei were observed on decellularized bone matrix. **(C)** H&E staining shows a lot of cells around and inside native bone matrix but few cells on decellularized bone matrix were seen **(D, E)**. **(F)** DNA quantification shows the dsDNA contents of native bone and decellularized bone matrix after decellularization. N = 3, mean ± standard deviation. **$p < 0.05$. The error bars represent standard deviation. DAPI: 4′,6-diamidino-2-phenylindole; H&E: Hematoxylin & eosin staining.

decellularization, the compressive strengths of DBM was 5.74 ± 0.43 MPa ($p > 0.05$; Figure 1F). There was no significant difference in the compressive strength between NBM and DBM. This suggests that the decellularization processes did not significantly alter the mechanical properties of the matrix and the mechanical strength of DBM was preserved well.

Nucleus characterization

To investigate if the porcine cells had been removed completely from the bone, quantitative and qualitative analysis methods were performed. DAPI staining reveals that there are many intact nuclei that can be clearly observed in the NBM (Figure 2A). However, most of cells had been removed in the DBM (Figure 2B). Furthermore, H&E staining shows the NBM possessed large number of cells, both in and around extracellular matrix (Figure 2C), but rather few nuclei were observed in DBM (Figure 2D). Some tiny residual cell nucleus fragments can be seen (Figure 2E), which confirmed that the decellularized method was effective. DNA quantitative test results show that dsDNA content in NBM was 677.17 ± 97.36 ng/ml and dsDNA content in DBM was 47.25 ± 9.33 ng/ml, indicating most cells were removed after decellularization ($p < 0.05$; Figure 2F).

Matrix components of NBM & DBM

The main organic component of bone matrix is collagen, especially collagen type I [34]. In order to test whether the integrity of collagen can be maintained during the decellularization process, quantitative and qualitative analysis

methods were carried out. Aniline blue staining showed that the blue line-like collagen fibers was still in DBM (Figure 3B), compared with those in NBM (Figure 3A), which meant that the collagen of bone matrix did not lose. Immunohistochemical staining was used specially to present how collagen type I remained. The striated dark brown markers on NBM (Figure 3C) and DBM (Figure 3D) were collagen type I. Although it is challenging to quantitatively analyze the content of collagen type I by immunohistochemical staining results, the brown color still demonstrates that collagen type I was maintained in the matrix after decellularization. We used Sirius red/Fast Green kit to stain total collagen and non-collagenous proteins in the matrix. Sirius Red specifically bound the collagens and Fast Green bound to non-collagenous proteins. The distribution and area of two kinds of colors are almost similar between NBM (Figure 3E) and DBM (Figure 3F). After staining, the stained components were extracted by the chemical solution in the kit according to the manufacturer's instruction. Quantitative test shows that there was no significant difference in the collagen content between NBM (2.19 ± 0.35 μg/section) and DBM (1.76 ± 0.38 μg/section; $p > 0.05$; Figure 3G). In addition, noncollagenous proteins contents were also similar between NBM (102.59 ± 23.84 μg/section) and DBM (93.56 ± 24.30 μg/section; $p > 0.05$; Figure 3H). This result suggested that both collagen and other noncollagen proteins were maintained. Both qualitative and quantitative analysis have shown that the decellularized method has the potential to maintain the major component of bone matrix, that being collagen. Other components of bone extracellular matrix were not specifically characterized in this study.

Morphologies of hMSCs on DBM & β-TCP scaffold

Figure 4A shows the appearance of a β-TCP scaffold. The pores of β-TCP scaffolds are interconnected (Figure 4B). The DBM and β-TCP scaffolds have the similar pore size and porous appearance, but the pores of DBM are slightly larger (Figure 1D, 4A & B). Based on the SEM, the estimated pore size of DBM is around 540 μm, while the estimated pore size range of β-TCP scaffolds was 450–550 μm (Figure 4B). SEM shows the morphologies of hMSCs cultured on DBM (Figure 4C) and a synthetic material β-TCP scaffold (Figure 4D) at day 7. The cells on DBM connected tightly with each other even to form a thick cell sheet covering the most surface of matrix (Figure 4C), while cells on β-TCP scaffolds were still growing to form a thicker layer (Figure 4D). These cell morphologies show that the DBM material can promote cell attachment and proliferation.

Cell attachment efficiency

The purpose of this experiment was to investigate the efficiency of the DBM and β-TCP scaffold to support cell attachment of hMSCs. In the preliminary attachment experiment, with the same number of initial cell seeding, the attachment efficiency on DBM was 93.92 ± 3.39% and the attachment efficiency on β-TCP scaffold was 60.91% ± 10.75 (Figure 4E). There were 1.5-times difference between them ($p < 0.05$), which implied that the pore structure and material property of DBM were more conducive for cell adhesion. In order to further verify the accuracy of this result, we seeded different initial cell numbers on the two types of scaffolds with 1.5-times difference in a second experiment (The seeding cell numbers on DBM were 1.5-times less than that on β-TCP scaffolds). Result shows that the cell attachment efficiency is similar on the two types of scaffolds. There is no significant difference ($[1.75 \pm 0.36] \times 10^4$ cells on DBM and $[1.72 \pm 0.23] \times 10^4$ on β-TCP scaffold; $p > 0.05$; Figure 4F).

Cell proliferation & differentiation of hMSCs

The dsDNA quantification shows the proliferation of hMSCs cultured on DBM and β-TCP scaffolds (Figure 5A). In general, the number of cells increased both on DBM and β-TCP scaffolds with time. From day 3 to 7, the growth rate of cells on DBM was faster than that on β-TCP scaffolds, especially on day 7 ($p < 0.05$), but they finally achieved the same rate of increase on day 14. The BCA protein assay on the two types of scaffolds also shows the same trend in cell proliferation (Figure 5B). It suggests that the DBM promoted cell proliferation faster than β-TCP. In order to evaluate early osteogenic differentiation of hMSCs on DBM and β-TCP scaffold, ALP activity test was applied (Figure 5C). The ALP activity was determined by normalizing ALP value of each sample to its protein concentration (Figure 5B). Overall, the ALP activity increased steadily from day 1 to 14 on DBM and β-TCP scaffolds. At day 14, cells on DBM demonstrated significantly higher ALP production than those on β-TCP scaffolds ($p < 0.05$).

To understand the expression of some osteogenic genes of hMSCs on DBM and β-TCP scaffolds, real-time PCR was implemented to assess four markers: *alp, runx2, bsp and oc* (Figure 5D). It is very surprising that the

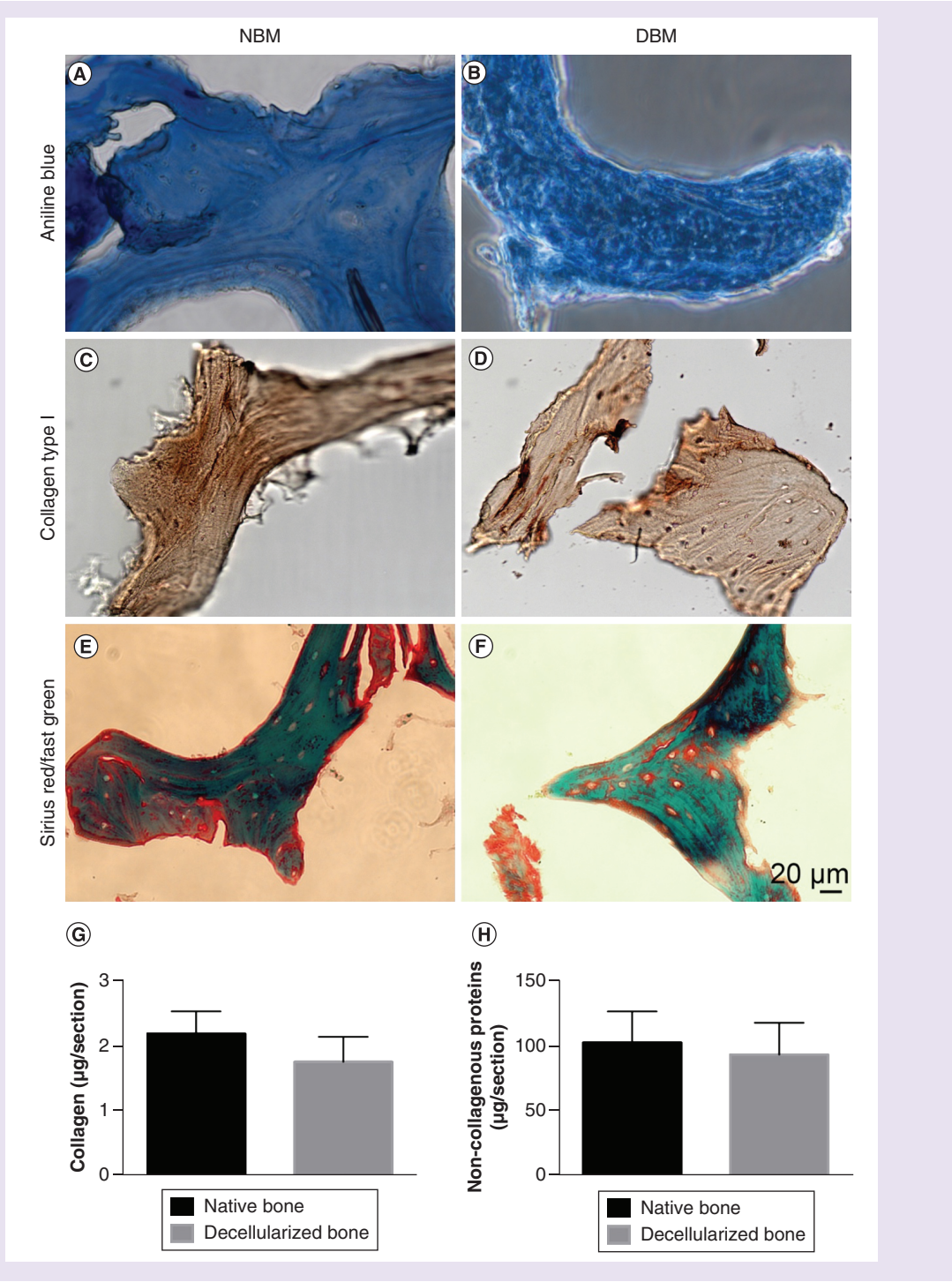

Figure 3. Bone matrix collagen characterization. Aniline blue staining shows collagen fibers in native bone matrix **(A)** and decellularized bone matrix **(B)**. Immunohistochemical staining specially presents collagen type I in native bone matrix **(C)** and decellularized bone matrix **(D)**. Sirius red/fast green staining for native bone matrix **(E)** and decellularized bone matrix **(F)**, red color bounds to collagens and green color bounds to non-collagenous proteins. Quantitative testing shows collagen contents **(G)** and non-collagenous proteins contents **(H)** between native bone matrix and decellularized bone matrix. N = 3, mean ± standard deviation. $p > 0.05$. The error bars represent standard deviation.
DBM: Decellularized bone matrix; NBM: Native bone matrix.

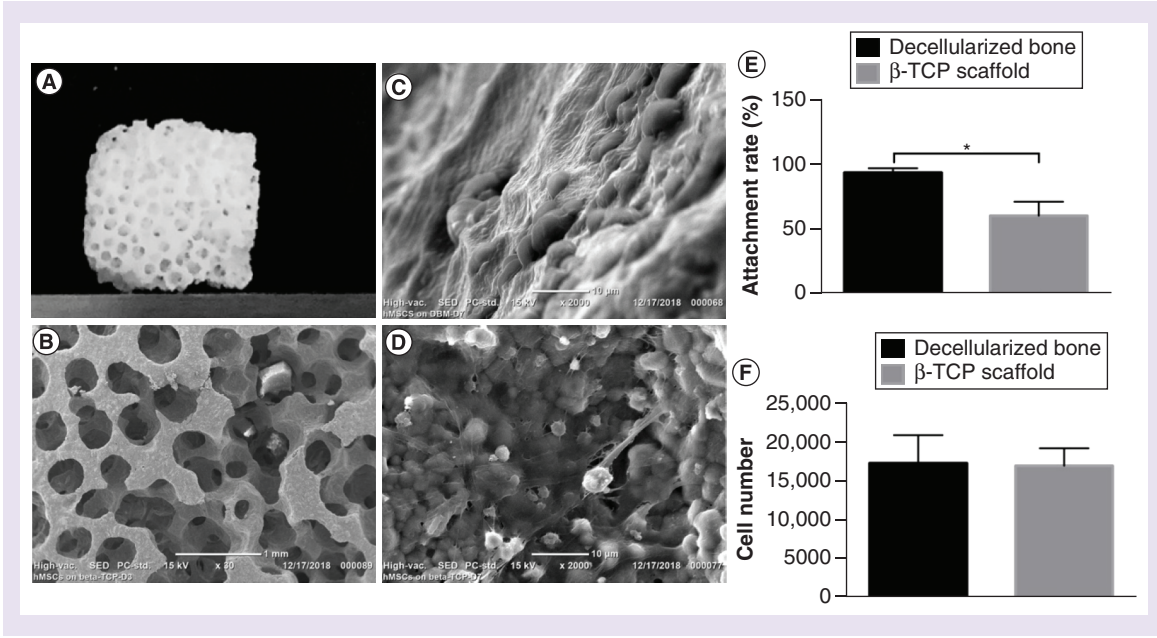

Figure 4. Cell attachments. (A) Overall appearance of β-TCP scaffold. **(B)** Scanning electron microscopy micrographs shows the pore morphology of β-TCP scaffold. Scanning electron microscopy shows the morphologies of hMSCs on decellularized bone matrix **(C)** and β-TCP scaffold **(D)** at day 7. The attachment rate of hMSCs attached on decellularized bone matrix and β-TCP scaffold after 4 h with equal initial cells **(E)**. N = 3, mean ± SD. *$p < 0.05$. The number of hMSCs attached on decellularized bone matrix and β-TCP scaffold after 4 h with initial cells as 1.5-times difference **(F)**. N = 3, mean ± SD. $p > 0.05$. The error bars represent SD.
hMSC: Human bone marrow mesenchymal stem cell; SD: Standard deviation.

expression of *alp, runx2* and *oc* genes did not show any difference between DBM and β-TCP scaffolds. DBM did not promote the expression of these genes compared with β-TCP scaffold. However, β-TCP scaffold promoted the gene expression of *bsp* at day 7, an early bone matrix gene *bsp* ($p < 0.05$). Afterward, it dramatically decreased. All in all, the four genes that are related osteogenesis did not express differently on the two types of scaffolds at most time points. However, very interestingly, the expressions of the four genes on DBM slightly increased from day 7 to 14 (red dotted-line), but on β-TCP scaffold slightly decreased from day 7 to 14 (dark blue dotted-line), although there is no significant difference in the increasing/decreasing magnitudes. These results suggested that β-TCP scaffold seemed to promote the gene expressions of osteogenic genes in advance than DBM. Meantime, these results show that the DBM did not show significant stimulation in the expression of osteogenic genes at early stage.

Discussion

There are extensive studies on bone-grafting biomaterials, regardless of synthetic or biological scaffold materials, for bone tissue regeneration. Decellularized matrix has been paid attention to study for tissue regeneration. Many sophisticated decellularization protocols had been developed in the past years to decellularize various tissue and organs. However, no matter physical, chemical, or enzyme-based decellularization methods, most of them can not satisfy the needs of completely removing cell nucleus and effectively maintaining the matrix components and structure [35]. In this study we took the advantages of those published decellularization protocols to develop a mild decellularization protocol to meet the needs of this procedure. The advantage of our new mild decellularization method is that this decellularization protocol combined mild chemical and enzymatic reagents to maximize the maintenance of the matrix components while effectively removing cell materials. We found that our modified decellularization method effectively removed cell nuclei, while overall maintaining the integrity and presence of matrix components.

Due to the complex anatomic geometry of craniofacial bone, it is challenging to implant bone grafts to repair the craniofacial bone defect. Therefore, flexibly shaping the bone scaffolds to fit the patient-specific bone defect

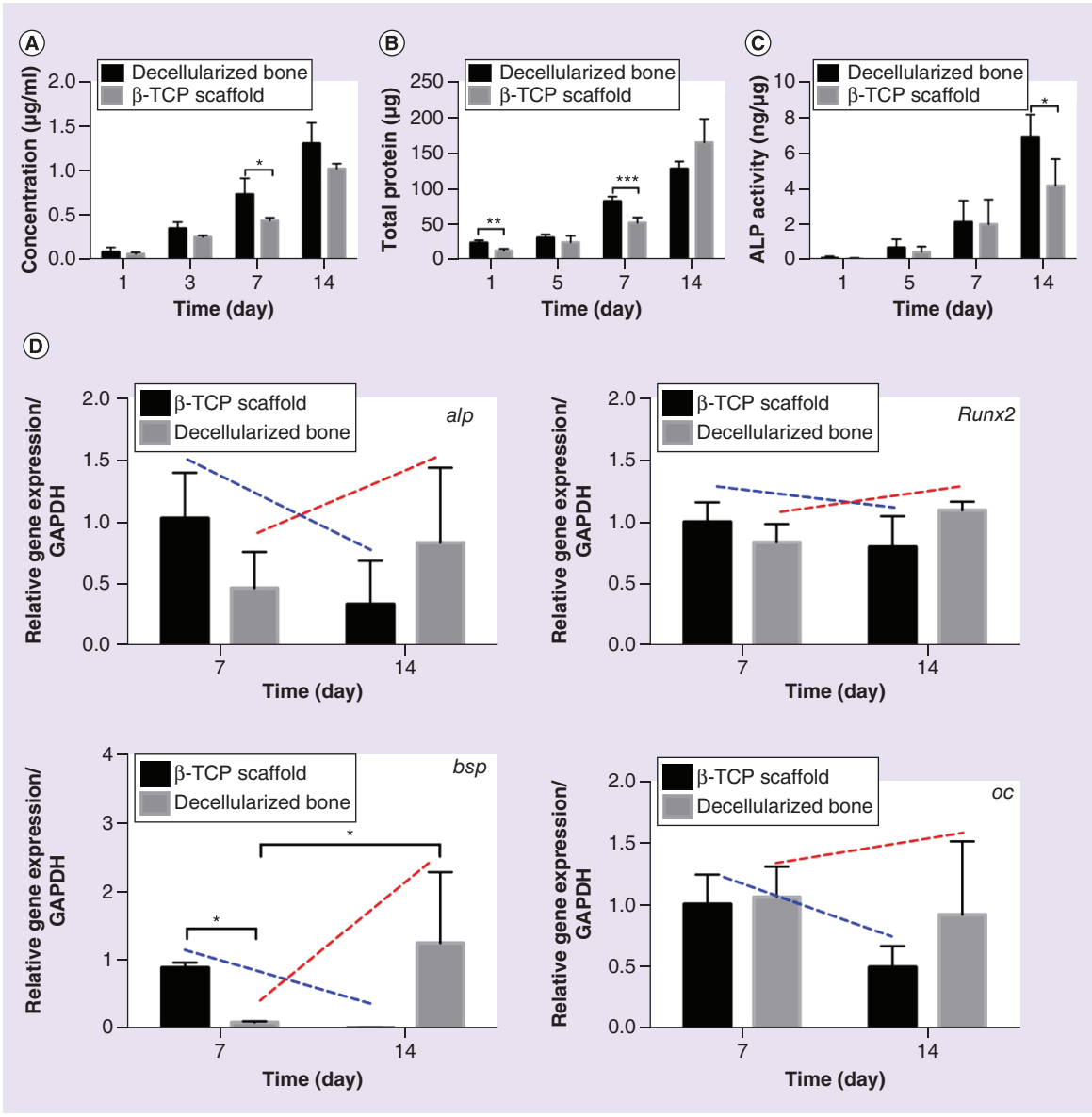

Figure 5. Cell proliferation of human bone marrow mesenchymal stem cells on decellularized bone matrix and β-tricalcium phosphate scaffold. (A) dsDNA contents of hMSCs on decellularized bone matrix and β-TCP scaffold. **(B)** Protein contents of hMSCs on decellularized bone matrix and β-TCP scaffold. **(C)** The ALP specific activity was determined by normalizing ALP value of each sample to its protein concentration. N = 3, mean ± SD. *$p < 0.05$. **(D)** Related osteogenic gene expression levels in hMSCs cultured on decellularized bone matrix and β-TCP scaffold, including *alp*, *runx2*, *bsp*, and *oc* genes. N = 3, mean ± SD. *$p < 0.05$. The error bars represent SD.
hMSC: Human bone marrow mesenchymal stem cell; SD: Standard deviation.

would be more demanding [36]. In previous studies decellularized bone matrices were often minced into bone particles or made into regular shape for bone defect [9,13,37,38]. Currently, most of bone filler biomaterials have limitations in providing macroscopic pores and structure of bone matrix for the repair of large bone defects. Although 3D printing technology is promising to produce anatomic shape of scaffolds for bone defects, the matrix components and porous structure cannot be same as the nature-derived decellularized bone matrix. In this study we demonstrated the promising potential of producing various shapes of the decellularized bone matrix to meet the challenge (Figure 1). Different shapes of the decellularized bone matrix indicate that this method robustly decellularized different shapes of large DBM to accommodate complex craniofacial defects for future clinically-translational applications.

In our preliminary experiments of this study, we tried to use multiple freeze–thaw cycles (from -196°C [liquid nitrogen] to 121°C [autoclave]) to decellularize the porcine bones [38]. Although freeze–thaw cycles can damage or destroy cell nuclei, they do not significantly maintain ECM proteins in tissues [10,39]. Our preliminary results (data not shown) showed that freeze–thaw process damaged the ultrastructure of ECM and made the decellularized matrix too weak and easily to be broken into powder. Our current mild decellularization process did not significantly damage the ECM of bone. At the same time, the mechanical strength of DBM was not remarkably altered (Figure 1F), which can provide structural support when implanted *in vivo*. Besides maintaining the mechanical and structural support, compared with synthetic bioceramic scaffolds, this decellularized matrix can provide natural bone matrix components for bone regeneration. For the ceramic scaffold that we used in this study as a control, it provides the inorganic ceramic component of a bone matrix. The main inorganic ceramic component in the scaffold after sintering is β -TCP, which is close to the inorganic component of nature bone matrix (hydroxyapatite), but β -TCP has a higher degradation rate than hydroxyapatite. Degraded Ca, P are beneficial for bone formation. Although α-TCP could appear in the scaffold as the transformation temperature of β-phase to α-phase is 1148°C, according to the previous studies [29], the sintering temperature at 1250°C for 3 h is a good condition to obtain β -TCP scaffolds, which can obtain similar mechanical strength of β-TCP scaffolds to that of cancellous bone matrix [31].

Besides the different components in DBM and β-TCP scaffold, there may be slight difference in pore size. We measured the pore size of the scaffolds from SEM images. In fact, the pores of DBM are not strictly round. They are elliptical and have big difference between pores, which is a natural consequence. However, the pores of β-TCP were generated by very round wax beads with a range of specific sizes. We used an established template casting method to make β-TCP scaffolds [30]. We filled wax beads in 24-well plates and casted β-TCP slurry to make the scaffolds. Although we cannot completely create exactly same internal geometrical shape, we have most similar scaffolds with similar pore size, morphology and internal geometries. Thus, the range of pores size of DBM and β-TCP scaffolds does not have statistically significant difference. However, it is worth to note that the different range of pore sizes may cause different surface area, which may affect other results. However, the slight difference in pore size between the two types of scaffolds may not have major effect on cell behavior than other parameters, like matrix components. To offset the slight difference in the internal geometry of β-TCP scaffolds and slight difference of pore size between the two types of scaffolds, three scaffolds per group for each test were used to achieve statistical significance.

One concern on decellularized bone matrix is its safety when used *in vivo* due to the residual DNA [40–42]. To improve the safety of scaffold materials, one of the key measures of decellularization is to remove cells as many as possible. In fact, most commercial decellularized biological scaffolds contain traces of residual DNA of less than 300 bp in length. Studies pointed out that it seems unlikely that any DNA fragments would be able to transmit disease into the host [41,43]. In this study, our modified decellularized method successfully removed approximately 94% of cellular materials. Triton X-100 is useful in removing cell residues from thicker tissues [44,45]. Sodium deoxycholate is a kind of anionic detergent [46]. The combination of the two reagents can effectively lyse and remove the cells from the porcine bone matrix [47]. After cell lysis, DNases I and RNases enzymes can cleave nucleic acid sequences and then remove nucleotides, specifically cell residues [10,48]. Although DNA quantitative result suggested that there were still some residual cell fragments, existing study reports showed that the residual rate of DNA is acceptable [11,41]. The rate in our decellularized bone matrix is lower. Even so, *in vivo* immune experiment is still needed to verify the safety of the decellularized bone matrix in our next step of this study.

Another key element in decellularization is the preservation of matrix components such as collagen. The bone ECM is composed of organic and inorganic components. The organic components are mainly composed of collagen type I, which accounts for 90% [49]. Collagen fibers are highly crosslinked and form the basic framework of ECM, which provides toughness, while also stimulates bone formation as well as cell attachment, proliferation and differentiation [50]. In this study, our decellularization process did not cause the loss of collagen component. The DBM can provide a three-dimensional structural support to cells and control their function, thus promoting tissue formation and regeneration. Besides, the presence of lipids in the native bone may affect the function of decellularized ECM. Therefore, we used 60°C warm water and 100% ethanol to effectively remove lipids from the native bone [51].

Biological scaffolds are one of the most popular bone scaffolds to induce bone regeneration with stem cells. In this study, we studied the cellular behavior of hMSCs on DBM and β-TCP scaffold respectively. The ability of cells to adhere to ECM is important in cell communication and regulation [52]. Studies have shown that cell

adhesion is associated with the following cellular activities, such as cell differentiation, cell cycle, cell migration and cell survival [53]. In our experiments, SEM on cell morphology show that more cells attached on the surface of DBM than β-TCP. This suggested that the native ECM components of DBM, for example, collagens are very conducive to the adhesion and growth of hMSCs. This result gave us a reasonable speculation that DBM could recruit host cells to promote tissue repair *in vivo* [54]. On the other hand, from cell proliferation experiments, we can see that the growth rate of hMSCs was relatively fast compared with β-TCP that has only Ca, P elements. Native ECM components are one of the better features of natural materials than synthetic ones. More cell attachment and growth would facilitate efficient bone regeneration.

ALP activity is a good indicator for early osteogenic differentiation of bone marrow mesenchymal stem cells. However, the ALP production of hMSCs in DBM was higher than that in β-TCP scaffold only after 14 days, not early stage (around 7 days in most studies), indicating that DBM does not have strong effect on early osteoblast differentiation of hMSCs compared with β-TCP. It is also surprising that DBM did not promote the gene expression of the *alp* gene. Similarly, DBM did not significantly promote the expression of other bone-related genes: *runx2, bsp* and *oc*. *Runx2* gene is a central gene of early osteogenesis that promotes the expression of other bone genes, such as *oc, bsp*, or *osteopotin*. We did not find that DBM significantly promoted the expression of these genes. On the contrary, it downregulated the expression of *bsp* at early stage compared with β-TCP. From the expressions of the four genes, we can see that the expressions of the four genes on β-TCP at the early stage decreased with time, but increased on DBM with time, although they do not have significant difference between the two types of scaffolds and between the two time points. From this result it is likely seems that the gene expressions of those genes on β-TCP occurred earlier than on DBM. All these above results could result from the reason of Ca and P ions. Large numbers of studies showed that Ca, P ions are very key ions for osteogenesis and bone formation [55]. β-TCP scaffold is biodegradable and Ca, P ions can be released from the scaffold at the early stage once it was incubated, which immediately stimulate the expression of osteogenic genes. This phenomenon was also observed in our previous study, where we found that fast degradation of channeled scaffolds promote osteogenesis as more Ca, P ions were released from the channels [56]. However, DBM is composed of collagen networks and hydroxyapatite that degrades slowly, resulting in slow release of Ca, P ions from DBM. Therefore, at the early stage, they did not significantly promote the ALP productivity and osteogenic gene expression but they promoted cell attachment and proliferation, because both collagen/other ECM organic components and hydroxyapatite have a better capacity to supporting cell attachment and growth [57]. This is an interesting finding, as we can see how important both components and degradation ability of a scaffold are for bone tissue regeneration. However, we do not know if this degradation rate would be similar to that *in vivo* condition.

Additionally, it is worth to note that in this study we used an osteogenic medium to culture hMSCs for osteogenic differentiation. It is possible that the stimulation effect of exogenous osteogenic growth factors in the medium on osteogenesis of hMSCs could cover the effect of matrix function on the osteogenesis. However, the level of the effect of the osteogenic medium in the experimental group and the control group could be the same. Subtracting the same effective level in the two groups, the significant difference that was observed in osteogenesis between the two groups should come from the matrix itself. This could be an intrinsic limitation when using an osteogenic culture medium to study the osteogenesis of stem cells on scaffolds. To overcome this limitation, we may consider to use non-osteogenic culture medium in the future. Based on current findings in this study, we can still see that DBM and β-TCP have their own advantages, as this is consistent with our previous studies on β-TCP, which showed that β-TCP scaffold has very promising potential to bone regeneration [58]. These results on the good properties of DBM would be further confirmed *in vivo* bone defect animal models in the next steps of our research.

Conclusion

In summary, we have successfully developed a new, mild decellularization method to obtain an acellular porcine-derived bone matrix. The cellular materials in the porcine bone were effectively removed and the mechanical strength, porous structure and collagen composition were maintained. Porcine-derived decellularized bone matrix has biocompatibility and can promote the proliferation of stem cells, providing promising potential for bone tissue regeneration, which has similar capacity of supporting osteogenesis to synthetic ceramic β-TCP scaffolds.

Translational perspective

The newly developed decellularization protocol is effective in decellularizing cell materials and maintaining the major matrix components. Current results show that the new porcine-derived DBM created in this study had

the promising potential in promoting cell adhesion and proliferation. The decellularization protocol maintain the biomimetic microenvironment and microarchitecture of native bone matrix for bone cells in terms of adhesion, survival and function, thus bringing promise for bone tissue regeneration. As the decellularization protocol can effectively produce bone matrix scaffolds with different shapes and sizes, the DBM bone scaffold has great potential to be used as a scaffold for bone tissue engineering and regenerative medicine purpose, especially in large bone defects or craniofacial bone defects. Future work should be performed to definitively prove osteogenesis of the decellularized bone matrix in animal models, and osteoinduction/osseointegration in a relevant *in vivo* model, for potential, translatable clinical applications. Besides the applications in bone tissue regeneration, this mimetic bone matrix can be used to build a bone cancer tissue-engineered model for mechanistic studies and drug screening of cancer bone metastasis, as the decellularized bone matrix maximumly maintain the structure and matrix components of a native bone.

Summary points

Main topics

- The repair of large craniofacial bone defect is still a challenge. Autografts, allografts, xenografts or synthetic scaffolds have been widely studied for bone tissue regeneration.
- Decellularized matrix is one of them and had shown many promising potentials in tissue regeneration.
- Here we developed a new mild decellularization method to prepare porcine-derived bone matrix scaffold for bone tissue engineering.

Results

- The decellularization protocol successfully removed more than 94% cells from porcine bones and maintained the major matrix components intact.
- *In vitro* cell culture experiments showed that the decellularized bone matrix promoted cell adhesion and proliferation, although it did not significantly promote the expression of osteogenic differentiation genes compared with the good osteoconductive β-tricalcium phosphate scaffolds.

Conclusion

- This study developed a new mild decellularization method to produce a biological bone matrix for potential application in bone tissue regeneration.
- This mild decellularization method has promising to decellularize bone matrix with different size from different sources.
- The decellularized bone matrix has similar function on cell behavior to osteoconductive β-tricalcium phosphate scaffolds.

Acknowledgments

The authors deeply appreciate the support of FAU high school imaging lab for the SEM.

Financial & competing interests disclosure

This study was supported by Florida Atlantic University internal start-up funds. The authors have no other relevant affiliations or financial involvement with any organization or entity with a financial interest in or financial conflict with the subject matter or materials discussed in the manuscript apart from those disclosed.

No writing assistance was utilized in the production of this manuscript.

Ethical conduct of research

The authors state that they have obtained appropriate institutional review board approval or have followed the principles outlined in the Declaration of Helsinki for all human or animal experimental investigations.

References

1. Nyberg EL, Farris AL, Hung BP *et al.* 3D-printing technologies for craniofacial rehabilitation, reconstruction, and regeneration. *Ann. Biomed. Eng.* 45(1), 45–57 (2017).
2. Petrovic V, Zivkovic P, Petrovic D, Stefanovic V. Craniofacial bone tissue engineering. *Oral. Surg. Oral. Med. Oral. Pathol. Oral. Radiol. Endod.* 114(3), e1–e9 (2012).
3. Broyles JM, Abt NB, Shridharani SM, Bojovic B, Rodriguez ED, Dorafshar AH. The fusion of craniofacial reconstruction and microsurgery: a functional and aesthetic approach. *Plast. Reconstr. Surg.* 134(4), 760–769 (2014).

4. Plum AW, Tatum SA. A comparison between autograft alone, bone cement, and demineralized bone matrix in cranioplasty. *Laryngoscope* 125(6), 1322–1327 (2015).
5. Tian T, Zhang T, Lin Y, Cai X. Vascularization in craniofacial bone tissue engineering. *J. Dent. Res.* 97(9), 969–976 (2018).
6. Baldwin P, Li DJ, Auston DA, Mir HS, Yoon RS, Koval KJ. Autograft, allograft, and bone graft substitutes: clinical evidence and indications for use in the setting of orthopaedic trauma surgery. *J. Orthop. Trauma* 33(4), 203–213 (2019).
7. Thrivikraman G, Athirasala A, Twohig C, Boda SK, Bertassoni LE. Biomaterials for craniofacial bone regeneration. *Dent. Clin. North Am.* 61(4), 835–856 (2017).
8. Lin Y, Huang S, Zou R *et al.* Calcium phosphate cement scaffold with stem cell co-culture and prevascularization for dental and craniofacial bone tissue engineering. *Dent. Mater.* 35(7), 1031–1041 (2019).
9. Liu M, Lv Y. Reconstructing bone with natural bone graft: a review of *in vivo* studies in bone defect animal model. *Nanomaterials (Basel)* 8(12), 999–1018 (2018).
10. Crapo PM, Gilbert TW, Badylak SF. An overview of tissue and whole organ decellularization processes. *Biomaterials* 32(12), 3233–3243 (2011).
11. Gilbert TW, Sellaro TL, Badylak SF. Decellularization of tissues and organs. *Biomaterials* 27(19), 3675–3683 (2006).
12. Badylak SF. Xenogeneic extracellular matrix as a scaffold for tissue reconstruction. *Transpl. Immunol.* 12(3–4), 367–377 (2004).
13. Lee DJ, Diachina S, Lee YT *et al.* Decellularized bone matrix grafts for calvaria regeneration. *J. Tissue Eng.* 7, 2041731416680306 (2016).
14. Cheng CW, Solorio LD, Alsberg E. Decellularized tissue and cell-derived extracellular matrices as scaffolds for orthopaedic tissue engineering. *Biotechnol. Adv.* 32(2), 462–484 (2014).
15. Pham QP, Kasper FK, Scott Baggett L, Raphael RM, Jansen JA, Mikos AG. The influence of an *in vitro* generated bone-like extracellular matrix on osteoblastic gene expression of marrow stromal cells. *Biomaterials* 29(18), 2729–2739 (2008).
16. Grayson WL, Frohlich M, Yeager K *et al.* Engineering anatomically shaped human bone grafts. *Proc. Natl Acad. Sci. USA* 107(8), 3299–3304 (2010).
17. You L, Weikang X, Lifeng Y *et al. In vivo* immunogenicity of bovine bone removed by a novel decellularization protocol based on supercritical carbon dioxide. *Artif. Cells Nanomed. Biotechnol.* 46(Suppl. 2), 334–344 (2018).
18. Marcos-Campos I, Marolt D, Petridis P, Bhumiratana S, Schmidt D, Vunjak-Novakovic G. Bone scaffold architecture modulates the development of mineralized bone matrix by human embryonic stem cells. *Biomaterials* 33(33), 8329–8342 (2012).
19. Mattioli-Belmonte M, Montemurro F, Licini C *et al.* Cell-free demineralized bone matrix for mesenchymal stem cells survival and colonization. *Materials (Basel)* 12(9), 1360–1372 (2019).
20. Bracey DN, Jinnah AH, Willey JS *et al.* Investigating the osteoinductive potential of a decellularized xenograft bone substitute. *Cells Tissues Organs* 207(2), 97–113 (2019).
21. Bracey DN, Seyler TM, Jinnah AH *et al.* A decellularized porcine xenograft-derived bone scaffold for clinical use as a bone graft substitute: a critical evaluation of processing and structure. *J. Funct. Biomater.* 9(3), 45–62 (2018).
22. Hashimoto Y, Funamoto S, Kimura T, Nam K, Fujisato T, Kishida A. The effect of decellularized bone/bone marrow produced by high-hydrostatic pressurization on the osteogenic differentiation of mesenchymal stem cells. *Biomaterials* 32(29), 7060–7067 (2011).
23. Schook LB, Collares TV, Darfour-Oduro KA *et al.* Unraveling the swine genome: implications for human health. *Annu. Rev. Anim. Biosci.* 3, 219–244 (2015).
24. Paulo Zambon J, Atala A, Yoo JJ. Methods to generate tissue-derived constructs for regenerative medicine applications. *Methods* 171(15), 3–10 (2019).
25. Badylak SF, Taylor D, Uygun K. Whole-organ tissue engineering: decellularization and recellularization of three-dimensional matrix scaffolds. *Annu. Rev. Biomed. Eng.* 13, 27–53 (2011).
26. Maliha SG, Lopez CD, Coelho PG *et al.* Bone tissue engineering in the growing calvaria using dipyridamole-coated, three-dimensionally-printed bioceramic scaffolds: construct optimization and effects on cranial suture patency. *Plast. Reconstr. Surg.* 145(2), 337e–347e (2020).
27. Kang Y, Kim S, Bishop J, Khademhosseini A, Yang Y. The osteogenic differentiation of human bone marrow MSCs on HUVEC-derived ECM and beta-TCP scaffold. *Biomaterials* 33(29), 6998–7007 (2012).
28. Kumar P, Vinitha B, Fathima G. Bone grafts in dentistry. *J. Pharm. Bioallied. Sci.* 5(Suppl. 1), S125–S127 (2013).
29. Liu Y, Kim JH, Young D, Kim S, Nishimoto SK, Yang Y. Novel template-casting technique for fabricating beta-tricalcium phosphate scaffolds with high interconnectivity and mechanical strength and *in vitro* cell responses. *J. Biomed. Mater. Res. A* 92(3), 997–1006 (2010).
30. Kang Y, Kim S, Khademhosseini A, Yang Y. Creation of bony microenvironment with CaP and cell-derived ECM to enhance human bone-marrow MSC behavior and delivery of BMP-2. *Biomaterials* 32(26), 6119–6130 (2011).
31. Kang Y, Scully A, Young DA *et al.* Enhanced mechanical performance and biological evaluation of a PLGA coated beta-TCP composite scaffold for load-bearing applications. *Eur. Polym. J.* 47(8), 1569–1577 (2011).

32. Kang Y, Kim S, Fahrenholtz M, Khademhosseini A, Yang Y. Osteogenic and angiogenic potentials of monocultured and co-cultured human-bone-marrow-derived mesenchymal stem cells and human-umbilical-vein endothelial cells on three-dimensional porous beta-tricalcium phosphate scaffold. *Acta Biomater.* 9(1), 4906–4915 (2013).
33. Livak KJ, Schmittgen TD. Analysis of relative gene expression data using real-time quantitative PCR and the 2(-Delta Delta C(T)) Method. *Methods* 25(4), 402–408 (2001).
34. Feng X. Chemical and biochemical basis of cell–bone matrix interaction in health and disease. *Curr. Chem. Biol.* 3(2), 189–196 (2009).
35. Porzionato A, Stocco E, Barbon S, Grandi F, Macchi V, De Caro R. Tissue-engineered grafts from human decellularized extracellular matrices: a systematic review and future perspectives. *Int. J. Mol. Sci.* 19(12), 4117–4196 (2018).
36. Bhumiratana S, Bernhard JC, Alfi DM *et al.* Tissue-engineered autologous grafts for facial bone reconstruction. *Sci. Transl. Med.* 8(343), 343ra383 (2016).
37. Rindone AN, Nyberg E, Grayson WL. 3D-printing composite polycaprolactone-decellularized bone matrix scaffolds for bone tissue engineering applications. *Methods Mol. Biol.* 1577, 209–226 (2018).
38. Gardin C, Ricci S, Ferroni L *et al.* Decellularization and delipidation protocols of bovine bone and pericardium for bone grafting and guided bone regeneration procedures. *PLoS ONE* 10(7), e0132344 (2015).
39. Patel N, Solanki E, Picciani R, Cavett V, Caldwell-Busby JA, Bhattacharya SK. Strategies to recover proteins from ocular tissues for proteomics. *Proteomics* 8(5), 1055–1070 (2008).
40. Yang JL, Yao X, Qing Q *et al.* An engineered tendon/ligament bioscaffold derived from decellularized and demineralized cortical bone matrix. *J. Biomed. Mater. Res. A* 106(2), 468–478 (2018).
41. Gilbert TW, Freund JM, Badylak SF. Quantification of DNA in biologic scaffold materials. *J. Surg. Res.* 152(1), 135–139 (2009).
42. Derwin KA, Baker AR, Spragg RK, Leigh DR, Iannotti JP. Commercial extracellular matrix scaffolds for rotator cuff tendon repair. Biomechanical, biochemical, and cellular properties. *J. Bone Joint Surg. Am.* 88(12), 2665–2672 (2006).
43. Badylak SF, Gilbert TW. Immune response to biologic scaffold materials. *Semin. Immunol.* 20(2), 109–116 (2008).
44. Meyer SR, Chiu B, Churchill TA, Zhu L, Lakey JR, Ross DB. Comparison of aortic valve allograft decellularization techniques in the rat. *J. Biomed. Mater. Res. A* 79(2), 254–262 (2006).
45. Willemse J, Verstegen MMA, Vermeulen A *et al.* Fast, robust and effective decellularization of whole human livers using mild detergents and pressure controlled perfusion. *Mater. Sci. Eng. C Mater. Biol. Appl.* 108, 110200 (2020).
46. Hudson TW, Liu SY, Schmidt CE. Engineering an improved acellular nerve graft via optimized chemical processing. *Tissue Eng.* 10(9–10), 1346–1358 (2004).
47. Yu BT, Li WT, Song BQ, Wu YL. Comparative study of the Triton X-100-sodium deoxycholate method and detergent-enzymatic digestion method for decellularization of porcine aortic valves. *Eur. Rev. Med. Pharmacol. Sci.* 17(16), 2179–2184 (2013).
48. Yang B, Zhang Y, Zhou L *et al.* Development of a porcine bladder acellular matrix with well-preserved extracellular bioactive factors for tissue engineering. *Tissue Eng. Part C Methods* 16(5), 1201–1211 (2010).
49. Florencio-Silva R, Sasso GR, Sasso-Cerri E, Simoes MJ, Cerri PS. Biology of bone tissue: structure, function, and factors that influence bone cells. *Biomed. Res. Int.* 2015, 421746 (2015).
50. Gentili C, Cancedda R. Cartilage and bone extracellular matrix. *Curr. Pharm. Des.* 15(12), 1334–1348 (2009).
51. Brown BN, Freund JM, Han L *et al.* Comparison of three methods for the derivation of a biologic scaffold composed of adipose tissue extracellular matrix. *Tissue Eng. Part C Methods* 17(4), 411–421 (2011).
52. Khalili AA, Ahmad MR. A review of cell adhesion studies for biomedical and biological applications. *Int. J. Mol. Sci.* 16(8), 18149–18184 (2015).
53. Huang S, Ingber DE. The structural and mechanical complexity of cell-growth control. *Nat. Cell. Biol.* 1(5), E131–138 (1999).
54. Papadimitropoulos A, Scotti C, Bourgine P, Scherberich A, Martin I. Engineered decellularized matrices to instruct bone regeneration processes. *Bone* 70, 66–72 (2015).
55. Li J, Liu C, Li Y *et al.* TMCO1-mediated Ca(2+) leak underlies osteoblast functions via CaMKII signaling. *Nat. Commun.* 10(1), 1589 (2019).
56. Wang X, Lin M, Kang Y. Engineering porous beta-tricalcium phosphate (beta-TCP) scaffolds with multiple channels to promote cell migration, proliferation, and angiogenesis. *ACS Appl. Mater. Interfaces* 11(9), 9223–9232 (2019).
57. Chou L, Marek B, Wagner WR. Effects of hydroxylapatite coating crystallinity on biosolubility, cell attachment efficiency and proliferation *in vitro*. *Biomaterials* 20(10), 977–985 (1999).
58. Yang J, Kang Y, Browne C, Jiang T, Yang Y. Graded porous beta-tricalcium phosphate scaffolds enhance bone regeneration in mandible augmentation. *J. Craniofac. Surg.* 26(2), e148–153 (2015).